Stability of the Gyroid Phase in Diblock Copolymers at Strong Segregation

Eric W. Cochran,[*,†] *Carlos J. Garcia-Cevera,*[‡] *and Glenn H. Fredrickson*[*,†,**]

Materials Research Laboratory, Department of Chemical Engineering, and Department of Mathematics, University of California, Santa Barbara, CA 93106.

Received:

[†]Materials Research Laboratory

[**]Department of Chemical Engineering

[‡]Department of Mathematics

*Authors for correspondence: ecochran@iastate.edu, ghf@mrl.ucsb.edu.

Abstract

We report high resolution self-consistent field theory (SCFT) calculations that show the gyroid phase, Q^{230}, to be stable in conformationally symmetric linear diblock copolymer melts prepared within the strong segregation regime, $\chi N = 100$, over a composition window of ~ 1.5%. This window broadens with the introduction of conformational asymmetry. The SCFT equations were solved using a novel pseudospectral approach with a plane wave basis and periodic boundary conditions. Saddle point field configurations were obtained using a semi-implicit Seidel relaxation algorithm. The modified diffusion equation was solved using a fourth-order backward differentiation formula and implicit treatment of the Laplacian operator. Our calculations are consistent with recent experimental observations of Q^{230} in strongly segregated diblocks.

The self-assembly behavior of linear AB diblock copolymers has been studied extensively over the past three decades, from both experimental and theoretical perspectives.[1-21] In the canonical theory, two independent parameters, the copolymer composition, *f*, and the degree of segregation, χN, govern the selection of the stable phase. While the three classical phases, lamellae (L); hexagonally packed cylinders (H); and body-centered spheres (Q^{229}), occupy the majority of the phase diagram, the double gyroid phase (Q^{230}), which occurs over only a narrow range of *f*, has occupied a disproportionate amount of researchers' attention.[13, 14, 18, 22-24] The intriguing topology of this network structure has inspired a diverse array of potential applications ranging from high-performance separation membranes to photonic crystals.

Unfortunately, the practical applicability of Q^{230} in the AB system appears limited due to the question of the stability of the phase in the strong-segregation regime. The majority of experimental reports of Q^{230} involved specimens prepared in the weak-to-intermediate segregation regime ($10 < \chi N < 40$).[14, 15, 18, 25] In addition, many of these tended to form hexagonally perforated lamellae (HPL) for larger χN, although this phase was later shown to be metastable.[12, 17, 18, 26] Moreover, studies that did in fact report Q^{230} at stronger segregation were prepared by solvent-casting, which is known to encourage the formation of kinetically trapped structures.[22, 24, 27-29] The theoretical community has also presented discouraging evidence. Olmsted and Milner[30, 31] argued using the strong-segregation theory (SST) of Semenov[7] that Q^{230} is unstable with respect to the classical phases, although this calculation imposed a wedge-shaped interfacial geometry that may be unrealistic; Likhtman and Semenov[32] performed an SST calculation without assuming an interfacial geometry and concluded that bicontinuous phases were stable only in the presence of added homopolymer. In 1994 Matsen and Schick presented a powerful, fully spectral implementation of Helfand's self-consistent field theory (SCFT)[1-5] that first demonstrated the stability of Q^{230} for $\chi N \leq 20$.[12] In 1996 Matsen and Bates continued the calculation to $\chi N = 40$, where the sharpening of the interfaces began to require a prohibitive number of basis functions and

caused numerical stability issues.[17] Based on the monotonic reduction of the Q^{230} stability region and the SST prediction, these researchers speculated that the Q^{230} window converged to a triple point with the classical L and H phases near $\chi N \sim 60$, possibly due to excessive packing frustration induced by the narrowing interfaces.[33] This notion was strengthened by subsequent corrections to the original SST, as well as analyses of the limiting behavior of SCFT as $\chi N \to \infty$.[19-21]

On the other hand, a recent experimental study by Davidock et al. presented a compelling case that Q^{230} does in fact persist well into the strong-segregation regime using a model system designed to have minimal kinetic barriers to equilibration.[34] Nonetheless, such evidence must be interpreted with a degree of caution since true thermodynamic equilibrium can be difficult to achieve even in intermediately segregated experimental systems.[35]

In the present communication we readdress this issue using SCFT, with the dual purpose of attending to the question of the high χN stability of Q^{230}, as well as showcasing significant advances in addressing the numerical hurdles encountered in solving the SCFT equations. The reader is directed elsewhere for a full description of the SCFT treatment of block copolymers.[1-5, 12, 36, 37] Here, we begin with the field-theoretic Hamiltonian H for an incompressible diblock copolymer melt:[36]

$$\frac{H[w_+, w_-]}{nk_BT} = \frac{1}{V}\int d\mathbf{r}\left[\frac{w_-^2}{\chi N} + w_+\right] - \ln Q[w_+, w_-] \qquad (1)$$

Here n is the number of chains, χ is the Flory segment-segment interaction parameter, V is the system volume, and N is the number of segments per copolymer; w_+ and w_- may be viewed as fluctuating pressure and exchange chemical potential fields, respectively. The pressure field enforces incompressibility, while the exchange field is conjugate to the composition pattern in the melt. Q is the single-chain partition function, which is computed according to $Q = \frac{1}{V}\int d\mathbf{r}\, q(\mathbf{r},1)$. The forward propagator $q(\mathbf{r},\mathbf{s})$ represents the statistical weight of segments located sN units along the chain contour

at point **r**, where $s = 0$ represents the tail of the A block and $s = f$ is the junction between the A and B blocks. Using the flexible Gaussian-chain model, q satisfies the modified diffusion equation (MDE):

$$\begin{aligned} \frac{\partial q(\mathbf{r},s)}{\partial s} &= R_g^2 \nabla^2 q(\mathbf{r},s) - w_i(\mathbf{r}) q(\mathbf{r},s) \\ i &= A; 0 \le s < f \\ i &= B; f \le s \le 1 \\ q(\mathbf{r},0) &= 1 \end{aligned} \tag{2}$$

where $w_A = (w_+ - w_-), w_B = (w_+ + w_-)$ and R_g is the unperturbed radius of gyration. The normalized segment density operators (volume fractions) ρ_A and ρ_B follow from functional derivatives of Q with respect to w_A and w_B and the familiar factorization property of q.

$$\begin{aligned} \rho_A(\mathbf{r}) &= -\frac{\delta \ln Q}{\delta w_A} = \frac{1}{VQ}\int_0^f \mathrm{d}s\, q(\mathbf{r},s) q^\dagger(\mathbf{r},s) \\ \rho_B(\mathbf{r}) &= -\frac{\delta \ln Q}{\delta w_B} = \frac{1}{VQ}\int_f^1 \mathrm{d}s\, q(\mathbf{r},s) q^\dagger(\mathbf{r},s) \end{aligned} \tag{3}$$

The reverse propagator, $q^\dagger(\mathbf{r},\mathbf{s})$, obeys (2) with $q^\dagger(\mathbf{r},1) = 1$.

Within mean-field theory, the free energy F corresponds to the Hamiltonian H evaluated at an appropriate saddle point field configuration $\left[w_+^*, w_-^*\right]$ in which the forces vanish, i.e.

$$\frac{\delta H}{\delta w_+} = \rho_A(\mathbf{r}) + \rho_B(\mathbf{r}) - 1 = 0 \tag{4}$$

$$\frac{\delta H}{\delta w_-} = \frac{2}{\chi N} w_-(\mathbf{r}) + (\rho_B(\mathbf{r}) - \rho_A(\mathbf{r})) + (2f - 1) = 0 \tag{5}$$

The calculation of saddle-point field configurations requires repeated evaluations of the forces, (4) and (5), which in turn through eq (3) rely on an accurate and efficient solution of the MDE (2). For strongly segregated systems, the sharpness of the A/B interface imparts a significant degree of stiffness to the SCFT equations (4)-(5), as well as the numerical evaluation of the propagators $q(\mathbf{r},\mathbf{s})$ and $q^\dagger(\mathbf{r},\mathbf{s})$. We address the latter issue by discretizing in space using collocation and a plane-wave basis, and solve the MDE by means of a semi-implicit method. The Laplacian

operator is treated implicitly with a fourth order backward differentiation formula (BDF4), whereas the source term is discretized explicitly using fourth order accurate Adams-Bashford[38]

$$\frac{25}{12}q_{n+1} - 4q_n + 3q_{n+1} - \frac{4}{3}q_{n-2} + \frac{1}{4}q_{n-3} = \Delta s\nabla^2 q_{n+1} - w(q_{n+1} + 4q_n - 6q_{n-1} + 4q_{n-2} - q_{n-3}) \qquad (6)$$

In this expression, q_{n+i} denotes $q(\mathbf{r},\mathbf{s}+i\Delta\mathbf{s})$, and Δs is the step size. The initial values required to apply this formula are obtained using backward Euler and Richardson's extrapolation. The resulting scheme is fourth order accurate and unconditionally stable. Moreover, it produces a fast decay of high frequency modes, which makes it an ideal candidate for stiff equations, in particular in combination with spectral collocation methods of the Fourier type.[38, 39] Using this scheme the average error in $q(\mathbf{r},\mathbf{1})$ was roughly 0.001% at $\chi N = 80$ and a step size of $\Delta s = 0.001$; second-order methods, such as the operator splitting scheme of Rasmussen and Kalosakas,[40] required $\Delta s < 10^{-5}$ to obtain the same level of accuracy.

We first calculated the saddle point configuration with $Ia\bar{3}d$ symmetry of an $f = 0.35$ diblock at $\chi N = 20$, using a function proportional to the first $Ia\bar{3}d$ harmonic (112) as the initial condition for w_-; w_+ was initially set to zero. (L and H calculations were initialized in an analogous manner.) For other coordinates in phase space the converged solution for an adjacent point served as an excellent initial condition. Saddle points were calculated using the semi-implicit Seidel (SIS) relaxation method proposed by Ceniceros and Fredrickson[41] to update the pressure field in Fourier-space while the exchange field was relaxed in real-space using an explicit forward Euler scheme. The period of the unit cell was optimized concurrently with the field relaxation by minimizing the microscopic stress,[42] also via an explicit scheme.

Each calculation utilized a step size of $\Delta s = 10^{-3}$ along the chain contour and a spatial resolution $\Delta x < 0.1\ R_g$ (for the 3D Q^{230} simulations this amounts to ~2 10^6 plane waves). The calculation proceeded iteratively until the magnitudes of the forces, (4) and (5), were at most $10^{-5}\ k_BT$ per chain. This degree

of precision was reached in roughly 2500 iterations, which for a single 3D gyroid calculation required roughly 72 hours of real-time using 32 Intel 3.06 GHz Xeon processors in parallel. This complement of numerical approaches has proven to an effective strategy for solving the SCF equations and remains stable even when the interfaces are both sharp and geometrically complicated as is the case in the present calculations.

In Figure 1 we plot the free energy per chain of the H and L phases with Q^{230} as the reference state. These curves show Q^{230} is stable with respect to these competing phases by no more than $0.007\ k_BT$ per chain; by comparison, $\Delta F_{DIS-Q^{230}} \approx 14\, k_BT$ at $\chi N = 100$, so the disordered phase is highly unstable at strong segregation. Figure 2 shows the corresponding phase boundaries, which are summarized in Table 1, on a revised diblock copolymer phase diagram. Our calculation of the composition boundaries of Q^{230} at $\chi N = 20$ coincide precisely with those reported by Matsen and Bates,[17] but deviate slightly at $\chi N = 40$, where the Matsen and Bates calculation began to encounter numerical difficulties. As χN is raised into the strong segregation regime, we find that the width of the stability window approaches $\Delta f \approx 0.015$ by $\chi N = 80$. In Table 2, we show that this window broadens significantly with the introduction of conformational asymmetry.

The stability of complex phases such as Q^{230} in block copolymers stems, in part, from the intermediate degree of interfacial curvature compared with neighboring L and H phases; this feature leads to an optimal degree of interfacial area and packing frustration.[33] This argument has been widely accepted for the presence of Q^{230} in the diblock phase diagram for weak-to-intermediate segregation. At strong segregation, packing frustration in Q^{230} should indeed be exacerbated by the narrowing of the interfacial thickness. This is likely the cause of the gradual contraction of the Q^{230} region from $\chi N = 20$ to $\chi N = 80$. However, our results show that near $\chi N = 80$ this exacerbation is nearly balanced with the

packing frustration of the H phase and the interfacial area of lamellae, indicating that Q^{230} survives over a narrow range of composition deep into the strong segregation regime. Conformational asymmetry evidently broadens this range, indicating that packing frustration is alleviated more efficiently in Q^{230} than in its competitors.

Here we caution that these results should not be construed as evidence *per se* that Q^{230} is stable in the strict $\chi N \to \infty$ limit (in the SST this limit is approached quite slowly, as $\chi N^{-1/3}$)[19], but rather as an indication that it might be. These calculations are in accordance with recent experimental evidence,[34] and demonstrate that the standard model for block copolymers contains the necessary physical ingredients to account for the presence of Q^{230} at strong segregation.

ACKNOWLEDGMENTS. The authors are grateful to Jeffrey Barteet, manager of the UCSB-MRL Computational Facilities. Extensive use was made of the MRL Facilities, supported by the National Science Foundation (NSF) under DMR-0520415, and the California Nanosystems Institute (CNSI) Computer Facilities, supported by NSF CHE-0321368. The work of C.J.G-C was supported by NSF grants DMS-0411504 and DMS-0505738, while G.H.F. acknowledges support from NSF DMR-0312097.

References

1. Helfand, E.; Tagami, Y. *Journal of Chemical Physics* **1972,** 56, (7), 3592-601.
2. Helfand, E. *Polymer Preprints (American Chemical Society, Division of Polymer Chemistry)* **1973,** 14, (2), 970-3.
3. Helfand, E. *Polymer Science and Technology (Plenum)* **1974,** 4, 141-56.
4. Helfand, E. *Journal of Chemical Physics* **1975,** 63, (5), 2192-8.
5. Helfand, E. *Accounts of Chemical Research* **1975,** 8, (9), 295-9.
6. Leibler, L. *Macromolecules* **1980,** 13, 1602-1617.
7. Semenov, A. N. *Soviet Journal of Experimental and Theoretical Physics* **1985,** 61, 733.
8. Ohta, T.; Kawasaki, K. *Macromolecules* **1986,** 19, (10), 2621-2632.
9. Bates, F. S.; Fredrickson, G. H. *Annu. Rev. Phys. Chem.* **1990,** 41, 525-57.
10. Vavasour, J. D.; Whitmore, M. D. *Macromolecules* **1992,** 25, (20), 5477-86.
11. Lescanec, R. L.; Muthukumar, M. *Macromolecules* **1993,** 26, (15), 3908-3916.
12. Matsen, M. W.; Schick, M. *Physical Review Letters* **1994,** 72, (16), 2660-2663.
13. Hajduk, D. A.; Harper, P. E.; Gruner, S. M.; Honecker, C. C.; Kim, G.; Thomas, E. L.; Fetters, L. J. *Macromolecules* **1994,** 27, 4063-4075.
14. Foerster, S.; Khandpur, A. K.; Zhao, J.; Bates, F. S.; Hamley, I. W.; Ryan, A. J.; Bras, W. *Macromolecules* **1994,** 27, (23), 6922-35.
15. Khandpur, A. K.; Foerster, S.; Bates, F. S.; Hamley, I. W.; Ryan, A. J.; Bras, W.; Almdal, K.; Mortensen, K. *Macromolecules* **1995,** 28, (26), 8796-8806.
16. Fredrickson, G. H.; Bates, F. S. *Annu. Rev. Mater. Sci.* **1996,** 26, 501-550.
17. Matsen, M. W.; Bates, F. S. *Macromolecules* **1996,** 29, (4), 1091-8.
18. Vigild, M. E.; Almdal, K.; Mortensen, K.; Hamley, I. W.; Fairclough, J. P. A.; Ryan, A. J. *Macromolecules* **1998,** 31, (17), 5702-5716.
19. Goveas, J. L.; Milner, S. T.; Russel, W. B. *Macromolecules* **1997,** 30, (18), 5541-5552.
20. Likhtman, A. E.; Semenov, A. N. *Europhysics Letters* **2000,** 51, (3), 307-313.
21. Matsen, M. W.; Gardiner, J. M. *Journal of Chemical Physics* **2003,** 118, (8), 3775-3781.
22. Urbas, A. M.; Maldovan, M.; DeRege, P.; Thomas, E. L. *Advanced Materials* **2002,** 14, (24), 1850-1853.
23. Schulz, M. F.; Bates, F. S.; Almdal, K.; Mortensen, K. *Phys. Rev. Lett.* **1994,** 73, (1), 86-9.
24. Hasegawa, H.; Tanaka, H.; Yamasaki, K.; Hashimoto, T. *Macromolecules* **1987,** 20, (7), 1651-62.
25. Bates, F. S.; Schulz, M. F.; Khandpur, A. K.; Foerster, S.; Rosedale, J. H.; Almdal, K.; Mortensen, K. *Faraday Discussions* **1994,** 98, 7-18.
26. Matsen, M. W.; Bates, F. S. *Journal of Polymer Science, Part B: Polymer Physics* **1997,** 35, (6), 945-952.
27. Aggarwal, S. L. *Polymer* **1976,** 17, 938.
28. Thomas, E. L.; Alward, D. B.; Kinning, D. J.; Martin, D. C.; Handlin, D. L., Jr.; Fetters, L. J. *Macromolecules* **1986,** 19, (8), 2197-202.
29. Spontak, M. F.; Smith, S. D.; Ashraf, A. *Macromolecules* **1993,** 26, (5), 956-962.
30. Olmsted, P. D.; Milner, S. T. *Physical Review Letters* **1994,** 72, (6-7), 936-939.
31. Olmsted, P. D.; Milner, S. T. *Physical Review Letters* **1995,** 74, (5-30), 829.
32. Likhtman, A. E.; Semenov, A. N. *Macromolecules* **1997,** 30, (23), 7273-7278.
33. Matsen, M. W.; Bates, F. S. *Macromolecules* **1996,** 29, 7641-7644.
34. Davidock, D. A.; Hillmyer, M. A.; Lodge, T. P. *Macromolecules* **2003,** 36, (13), 4682-4685.
35. Lipic, P. M.; Bates, F. S.; Matsen, M. W. *Journal of Polymer Science. Part B, Polymer Physics* **1999,** 37, 2229-2238.

36. Fredrickson, G. H., *The Equilibrium Theory of Inhomogeneous Polymers*. Oxford University Press: Oxford, 2006.
37. Matsen, M. W. *Journal of Physics: Condensed Matter* **2002,** 14, (2), R21-R47.
38. Lambert, J. D., The initial value problem. In *Numerical Methods for Ordinary Differential Systems.*, John Wiley & Sons: Chichester, 1991.
39. Ascher, U. M.; Ruuth, S. J.; Spiteri, R. J. *Applied Numerical Mathematics* **1997,** 25, 151-167.
40. Rasmussen, K. O.; Kalosakas, G. *Journal of Polymer Science, Part B: Polymer Physics* **2002,** 40, (16), 1777-1783.
41. Ceniceros, H. D.; Fredrickson, G. H. *Multiscale Modeling and Simulation* **2004,** 2, (3), 452-474.
42. Barrat, J.-L.; Fredrickson, G. H.; Sides, S. W. *Journal of Physical Chemistry B* **2005,** 109, 6694-6700.

Tables

Table 1. Phase boundaries of Q^{230} in AB diblocks in the strong segregation regime.

χN	$f_{H/Q^{230}}$	$f_{L/Q^{230}}$	Δf
20	0.338_0	0.375_0	0.037_0
40	0.315_3	0.336_7	0.021_7
60	0.311_3	0.328_5	0.017_2
80	0.308_8	0.324_2	0.015_4
100	0.306_5	0.321_9	0.015_3

Table 2. Phase boundaries of Q^{230} in AB diblocks with conformational asymmetry.

χN	b_A/b_B[a]	$f_{H/Q^{230}}$	$f_{L/Q^{230}}$	Δf
40	0.67	0.411_2	0.438_1	0.027_0
40	1.00	0.315_3	0.336_7	0.021_7
40	1.50	0.239_4	0.265_8	0.026_4
80	0.67	0.422_1	0.442_9	0.020_8
80	1.00	0.308_8	0.324_2	0.015_4
80	1.50	0.207_9	0.234_5	0.026_6

[a]The ratio of the Kuhn segment length of blocks A and B, which is a measure of the conformational asymmetry.

Figures

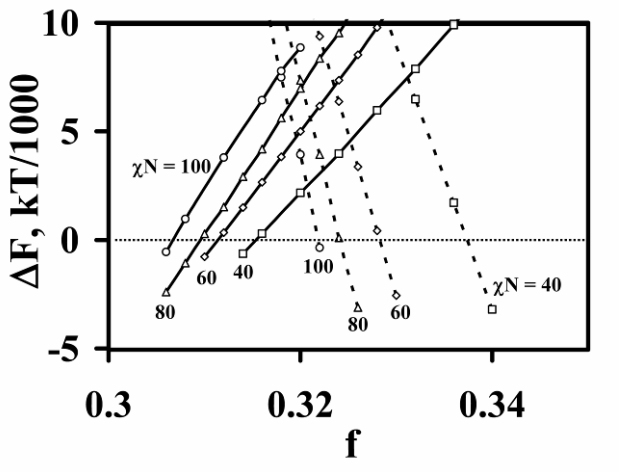

Figure 1. Stability of the H and L phases with respect to Q^{230} at various degrees of segregation: $\chi N =$ 40 (□), 60 (◇), 80 (△), and 100 (○). Solid ($\Delta F = F_H - F_{Q^{230}}$) and dashed ($\Delta F = F_L - F_{Q^{230}}$) curves are provided to guide the eye.

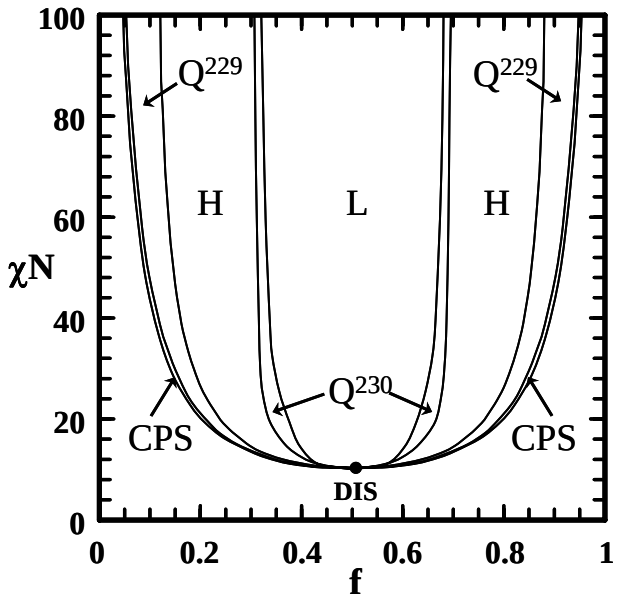

Figure 2. Revised diblock copolymer phase diagram, adapted from ref 17, that accounts for the Q^{230} phase boundary calculations that appear in Table 1. Q^{229} and CPS refer to the spherical phases with $Im\bar{3}m$ and close-packed (fcc or hexagonal) symmetry, respectively.

FOR TABLE OF CONTENTS USE ONLY